Full paper

Diffusion Induced Effects on Geometry of Ge Nanowires

S. J. Rezvani*[a,b], N. Pinto[a,d], L. Boarino [b], F. Celegato [b], L. Favre [c] and I. Berbezier [c]

We report diffusion induced germanium nanowires growth and its dependence on Ge evaporation flux. Wires show a growth rate (dL/dt) in agreement to the previously reported models, but detection of anomalies in grown wires, may indicate the prevalence of the direct Ge impinging effect in large diameter wires. Additionally, we demonstrate that change in deposition flux could directly affect the diffusion length of the Ge adatoms on the wires sidewalls. This turns to modify the geometry of the grown wire by introducing a lateral growth starting from the base of the wire. A detailed understanding of the deposition flux effect on the growth and geometry of wire will result in an improved knowledge of physical properties of wires.

1 Introduction

Germanium nanowires (NW) with their enhanced mobility have possibility to improve the electrical and optical properties of many devices and be used in photovoltaics[1,2], electronics[3–5] and sensors[6,7] applications. Out of different methods available to grow semiconducting nanowires, vapor liquid solid (VLS), described by Wagner and Ellis, is the mechanism well studied[8] which can result in a flexible and controllable one-dimensional NWs growth with a diameter similar to that of metal particle. There are several models available for the VLS mechanism via MBE, which suggest a diffusion induced (DI) growth. They consider that in MBE, the metal droplet does not act as a catalyst but as a seed for diffused adatoms reaching the droplet from the substrate as well as from direct impinging to the wires sidewall[9–11]. These models defines the growth rate of wire in direct dependence to the adatom diffusion length[12] and a V dependence as $V^{-\theta}$ with $\theta = 0.5$, V being the deposition flux[10]. Moreover, wires orientation is suggested to be radius dependent in VLS growth as well[13], while recent works show that other factors also influence the growth regime[14,15]. In recent years, several studies are carried out on chemical deposition of the semiconductor nanowires, in particular silicon[16–18]. However, there are few experimental investigations available on growth mechanism and geometrical frustrations of germanium NWs grown by MBE, that takes into account the DI-VLS mechanism. Furthermore the effect of the deposition flux (and the diffusion length) of the evaporated material on geometrical properties of the grown wires is not clearly understood yet.

A detailed knowledge of the deposition flux effect on the growth mode and geometry of wire can lead to a better understanding of the growth process, resulting in a more controlled fabrication of the wires. Here we report the structural and geometrical properties of the germanium nanowires grown at different deposition flux conditions using high-resolution electron microscopy. We also demonstrate not only a change in the vertical growth rate (dL/dt) but also a strong geometrical frustration due to the adatom diffusion. These frustrations can change the shape of the wire, resulting in an irregular geometry.

[a] School of Science and Technology, University of Camerino,I-62032 Camerino, Italy; Tel:0039737402528,E-mail: seyedjavad.rezvani@unicam.it
[b] Istituto Nazionale di Ricerca Metrologica, INRiM, I-10135 Torino, Italy
[c] IM2NP - UMR CNRS, Aix-Marseille Universite, France
[d] INFN, Sezione di Perugia, Via A. Pascoli, I-06123 Perugia, Italy

2 Experiment

Samples have been grown in a MBE chamber with base pressure of 3×10^{-11} Torr, by using Knudsen cells. Ge(111) wafers have been ultrasonically cleaned in methanol and trichloroethylene, followed by removal of the native oxide using sulfuric acid and dipped in $H_2O_2 : NH_3OH : H_2O$ for re-oxidation. Previous to the Au deposition, wafer has been annealed at 400 $°C$ for 30 minutes to remove the overgrown oxide. Then, in vacuum samples have been moved to the Au deposition and a thin Au layer (0.3 nm) was thermally evaporated at room temperature. Samples were returned to the MBE chamber immediately and annealed at 600 $°C$ for 15 minutes in order to achieve nano-droplets and then cooled down rapidly to 430 $°C$ for Ge nanowires growth. All the samples have been prepared in a way to have the same equivalent thickness of germanium. Samples have been studied using high-resolution scanning electron microscopy (HRSEM), scanning transmission electron microscopy (STEM) and high-resolution transmission electron microscopy (HRTEM).

3 Results and discussion

Nanowires grown at $V = 0.02$ nm/s of germanium deposition flux are shown in figure 1. High resolution electron microscopy (HRSEM) images evidence tilted wires with three different directions making an angle of 120° with each other and 54.7° with the substrate, also reported previously[19]. High-resolution transmission electron microscopy (HRTEM), also reveals that NWs are single crystalline, defect free and dominantly in $\langle 110 \rangle$ and $\langle 211 \rangle$ orientation (Figure 2) as reported for Ge NWs[20]. Au droplets are always on a tilted facet at the

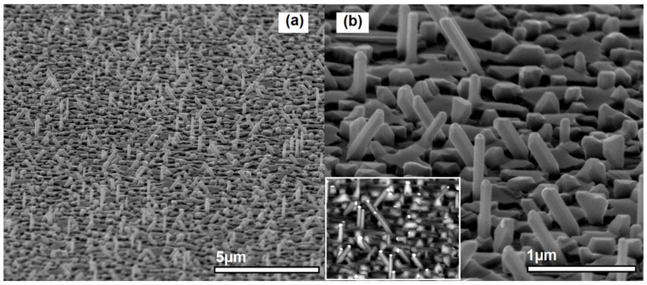

Fig. 1 a) Large scale HRSEM images of the wires grown at V = 0.02 nm/s. b) High magnification HRSEM image of the same sample, with back scattering electron diffraction (BSED) inset image. Bright point at the wire tip indicates the gold droplet position. The apparent vertical wires are due to the artifact caused by tilting of the sample to improve the visibility.

tip, from $\{100\}$ to $\{111\}$, due to the tendency to decrease the interface free energy σ_i according to Neumann triangle relation[21] $\frac{\sigma_{Ge}}{sin\phi_s} = \frac{\sigma_{Au}}{sin\beta} = \frac{\sigma_i}{sin\phi_l}$ (figure 2c,d). Moreover, wires show irregular cross sections close to a rhombohedral[23] one, in contrast to the data reported for Ge NWs grown by chemical vapor deposition[19,24]. It may be considered as an asymmetric two faceted cross section mode, extended by Au droplet oscillation[22]. In the micrographs taken by STEM (as well as back scattering STEM), we could not detect any Au clusters on surface of wires (Figure 3a), as expected according to the data reported in literature for silicon[25]. However, the presence of facets suggests the Au diffusion through the wire surface[26] which may indicate that clusters were not detected due to sensitivity limit of the technique. Additionally, the change in diameter of few NWs (Figure 3b), indicates the ripening during the growth[27]. NWs show a smooth surface structure without high frequency sawtooth faceting, also detected in silicon[28,29]. Howbeit, there are steps mostly in large diameter NWs (Figure 3, main panel), along the length of wire, which can be considered as sawtooth faceting with very low frequency. This effect can be due to change in the droplet contact angle (discussed above) related to the wire diameter by[30] $\sigma_i \simeq \frac{D}{\Lambda}$ in which Λ is the wavelength of the steps and D is the diameter of the wire. The wavelength tends to increase as D decreases confirming a lowering of σ_i.

The ratio of the length, L, to the radius, r_w, of the wires grown by flux of V = 0.02 nm/s is plotted in figure 4a which, reveals a behavior in agreement to the DI model described by[12]

$$\frac{dL}{dt} = 2\Omega R(1 + \frac{L_f}{r_w}) \quad (1)$$

For $L >> L_f$, in which R is the flux on the sidewall of the wire, Ω is the atomic volume of the deposited material and L_f is the diffusion length. However, fitting the data of the length vs radius of the wires grown at V = 0.02 nm/s gives a value

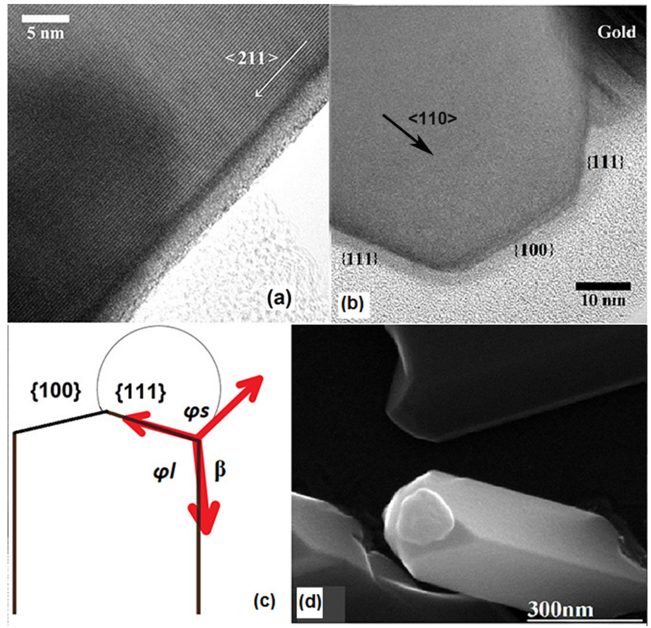

Fig. 2 a, b) HRTEM images of Ge NWs grown at V = 0.02 nm/s showing the dominant orientations of $\langle 110\rangle$ and $\langle 211\rangle$. NWs are single crystalline and defect free. b) Wire shows two facets at the tip with the Au droplet, sitting on $\{111\}$ facet, regardless of the orientation of the wire. c) Schematic of the faceting at the tip to minimize the interface energy; d) HRSEM view of the $\{111\}$ facet on which Au droplet sits. The image shows an irregular cross section close to rhombohedra.

of $L_f = 100 \pm 10$ nm. This value is lower than the experimental one of L_f = 126 nm, reported before using deposition flux of 0.013 nm/s at 430 °C with other similar deposition parameters[20]. This difference in L_f values, may indicate a dependence of the diffusion length of adatoms on deposition flux, as will be discussed in detail below. Albeit, it is worth mentioning that we detected anomalies of a density of $\sim 5\%$ in grown wires, which are neglected in the graph, such as the one shown in the figure 4b. These includes NWs having high lengths and large diameters. This morphology can be due to either modified diffusion of Ge adatoms caused by terraced structures on the surface or the Gibbs-Thompson effect[31] which causes the prevalence of direct impinging of the Ge adatoms on the sidewall of large diameter wires. In fact, in wires longer than the surface diffusion length of the adatoms, the Ge diffusion from the sidewalls can become strongly dependent on the wires perimeter. Hence, the wires with larger diameter can receive more adatoms from the sidewall and grow faster[32,33]. This effect is also dependent on the deposition time[34], which in our case, with a relatively low growth temperature, is long enough to trigger the effect.

Considering the calculated diffusion length mentioned pre-

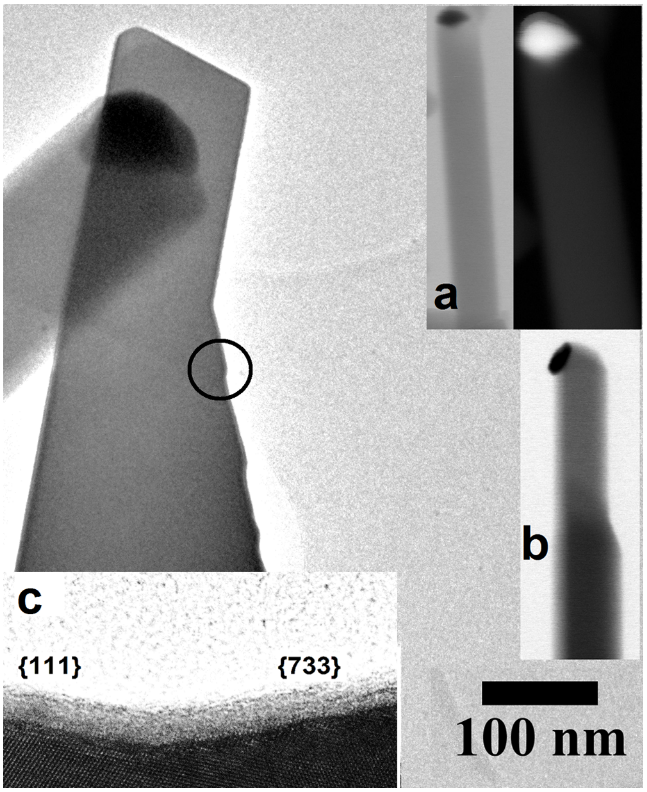

Fig. 3 Main panel: HRTEM image of a single wire showing low frequency faceting. Another wire with an Au droplet on the tip can be seen in the back as well. a) Left: STEM image of a wire and BSED of the same wire (right) demonstrate absence of the Au clusters on the sidewalls and no high frequency saw tooth structure on the surface. b) STEM of another wire, showing faceting and reduction of the Au droplet size, suggesting the diffusion of Au on the surface (ripening), although not detectable in the BSSTEM. c) Magnification of the circled area in the main panel which shows $\{111\}$ and $\{733\}$ facets.

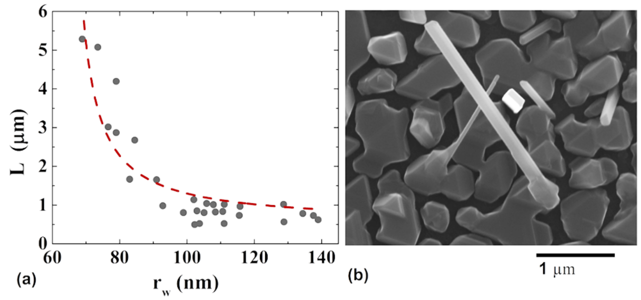

Fig. 4 a) Relation between length and radius of the NWs grown at V = 0.02 nm/s. Fitting, using equation (1) of the main text, gives the value of $L_f = 100 \pm 10$ nm. b) SEM image of NWs showing anomalies in radius dependence of the length. These anomalies are detected in large diameter wires, which are not considered in the graph of panel (a).

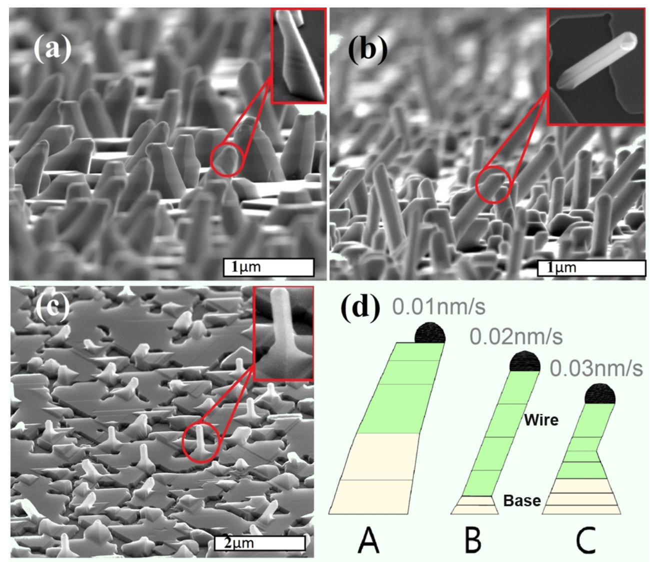

Fig. 5 SEM images of three samples prepared at: a) V = 0.01 nm/s. NWs with the irregular geometry (faceted) evidence the presence of a sizeable lateral growth (also visible in the inset). b) V = 0.02 nm/s, a minimal base expansion is evident; c) V = 0.03 nm/s, a cone shaped expanded base is visible. All the samples show a vertical growth rate in accordance to the diffusion length, related to the deposition flux. d) Schematic of the estimated geometry of the case (a), (b) and (c), respectively. Insets are the high magnification of the selected wires, detailing their geometry

viously, we investigated the effect of the Ge evaporation flux, being a relevant parameter, on the NWs growth. Wires formed with evaporation flux of V = 0.02-0.05 nm/s are shown in figure 5. At V = 0.02 nm/s (Figure 5 b) wires present the abovementioned features, with a minimal expansion of the base, as reported by Schmidt et al[13]. At V = 0.03 nm/s (Figure 5c), NWs evidence an expansion of the base even farther in addition to shorter length, while a flux of V = 0.01 nm/s (Figure 5a) produces highest lateral expansion, leading to an irregular geometry. The nature of resulting geometry features are not completely clear yet. However, the geometry transitions may be explained invoking a mechanism, dependent on the Ge adatoms diffusion length, by considering that L_f depends on V as in $L_f \simeq V^{-\theta}$[35].

Fitting the dependence of the NW length on V (Figure 6a), gives a value of $\theta = 0.35 \pm 0.05$ which is in agreement with the value of $\theta = 0.3$ expected for the surface self diffusion of Ge[36,37]. However, it is worth mentioning that removing the value, corresponding to NWs with irregular geometry (V = 0.01 nm/s) will increase the θ value to $\theta = 0.43 \pm 0.02$, which is in quite reasonable agreement with the expected value $\theta = 0.5$ by the model[38]. The above mentioned results may suggest a limited growth mechanism for NWs with irregular geometry, as will be discussed afterwards. Taking into account the above mentioned dependence of L_f on V, a deposition flux of V = 0.02 nm/s (Figure 5b), imposes an equilibrium between the flux of the Ge adatoms diffused on the substrate and flux of Ge adatoms directly impinged on the sidewall, with their relative diffusion length. Thus, the wire starts to grow vertically with the expected base expansion. For the higher rates, such as V = 0.03 nm/s (Figure 5c), despite the increase in flux of Ge adatoms arriving to the collecting area, a lateral growth takes place close to the base due to low L_f of Ge adatoms arriving to the base. This can cause further expansion of the base and formation of a cone like structure, which was predicted by the model for high fluxes[39]. Additionally wires show lower vertical growth rate, relative to the assigned L_f. Further raise of flux to V= 0.05 nm/s, increases the base expansion and reduces the wire length due to the decrease in L_f. Besides, the adatoms will be trapped in the non-activated islands (without Au droplet) on the surface, before reaching the wire, and the islands start coalescing together (Figure 6b) and finally forming a 2D film.

However, Ge NWs resulting from the flux of V = 0.01 nm/s requires a different interpretation since their particular geometry cannot be explained solely by the mechanism, mentioned above. Decrease of the deposition flux to V = 0.01 nm/s (Figure 5a), revealed a lateral overgrow on the sidewall which is in contrast to the model, proposing less base expansion for lower deposition flux. This morphology, though not clear yet, can be a limited growth mechanism due to a combination of L_f increase caused by a reduction of the flux, as well as an increase in the ratio θ_l/θ_f of the so called activities of adatoms in the droplet, θ_l, and on the sidewalls, θ_f, proposed by Dubrovskii et al.[34,38]. Increase in the diffusion length results in a longer wire for lower deposition rate. However, at a given length, the possibility of maximized adatom activity in the droplet compared to the sidewalls may turn $\theta_l/\theta_f > 1$, which will change the sign of the diffusion. This can initiate an additional Ge flux by an alteration in the direction of the diffusion from the droplet to the sidewalls, leading to a radial growth. Having a high adatom flux, can lead to an extensive homogeneous growth along the total length of the wire. Consequently, by increase in the radial growth, the faceting increases and an irregular shape will result[40]. These faceting can be the effect of the periodic oscillation of the droplet angle[30] or Au partially diffused on the sidewalls and formed a thin surface layers during the NW growth proposed by Oehler et al.[40] which in the sensitivity limit of our system could not be detected. Finally, our study has shown a maximum in the spatial density of wires vs evaporation flux at this specific growth temperature, corresponding to the value of V=0.02 nm/s (Figure 6c).

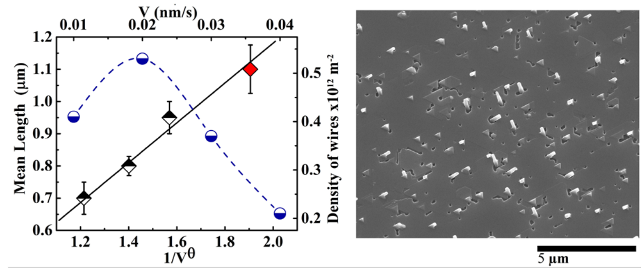

Fig. 6 (right) Black symbols: linearized dependence of the NWs mean length vs evaporation flux. Fitting (continuous line) gives the value of $\theta = 0.35 \pm 0.05$ considering all the points while gives the value of $\theta = 0.43 \pm 0.02$, removing the NWs with irregular shape (red filled symbol). Blue symbols: dependence of the spatial density of the wires vs the evaporation flux. The dashed curve is a guide for eyes only. (right) Wires grown at V = 0.05 nm/s, showing formation of a 2D layer on the surface and coalescing of the wires base with the 2D structure. Length of the wires are also in accordance to the diffusion length, related to the deposition flux.

4 Conclusion

Germanium nanowires hae been grown by vapor-liquid-solid (VLS) method using size controlled Au droplets by molecular beam epitaxy (MBE). Nanowires have shown a growth according to the diffusion induced mechanism with irregularities, which can represent the size dependency of the model. Experimental results show also, a dependency of the sidewall adatom diffusion length on evaporation flux. This dependency changes the growth mode and geometry of the wire to an immense range. We have proposed a mechanism, which can explain to some extent the mechanism involved in growth parameter effect. However, further studies are necessary in order to establish a model that explains the radial and vertical growth equilibrium.

5 Acknowledgement

This work is partially supported by Nanofacility Piemonte, a laboratory supported by Compagnia di San Paolo Foundation. We would like to thank G. Amato, L. Morresi, R. Gunnella and A. Di Cicco for helpful discussions.

References

1 B. Tian, X. Zheng, T. J. Kempa, Y. Fang, N. Yu, G. Yu, J. Huang and C. M. Lieber, *Nature*, 2007, **449**, 885–9.

2 L. Tsakalakos, J. Balch, J. Fronheiser, B. a. Korevaar, O. Sulima and J. Rand, *Applied Physics Letters*, 2007, **91**, 233117.

3 N. J. Quitoriano and T. I. Kamins, *Nano letters*, 2008, **8**, 4410–4.

4 Y. Cui, Z. Zhong, D. Wang, W. U. Wang and C. M. Lieber, *Nano letters*, 2003, **3**, 149–152.

5 Z. Zhong, D. Wang, Y. Cui, M. W. Bockrath and C. M. Lieber, *Science (New York, N.Y.)*, 2003, **302**, 1377–9.

6 Y. Cui, Q. Wei, H. Park and C. M. Lieber, *Science (New York, N.Y.)*, 2001, **293**, 1289–92.

7 Z. Li, Y. Chen, X. Li, T. I. Kamins, K. Nauka and R. S. Williams, *Nano letters*, 2004, **4**, 245–47.

8 R. S. Wagner and W. C. Ellis, *Applied Physics Letters*, 1964, **4**, 89.

9 V. G. Dubrovskii, N. V. Sibirev, J. C. Harmand and F. Glas, *Physical Review B*, 2008, **78**, 235301.

10 V. Dubrovskii, G. Cirlin, I. Soshnikov, a. Tonkikh, N. Sibirev, Y. Samsonenko and V. Ustinov, *Physical Review B*, 2005, **71**, 205325.

11 V. Dubrovskii, N. Sibirev, G. Cirlin, J. Harmand and V. Ustinov, *Physical Review E*, 2006, **73**, 021603.

12 J. Johansson, C. Svensson, T. Mårtensson, L. Samuelson and W. Seifert, *The journal of physical chemistry. B*, 2005, **109**, 13567–13571.

13 V. Schmidt, S. Senz and U. Gösele, *Applied Physics A*, 2004, **80**, 445–450.

14 A. Lugstein, M. Steinmair, Y. Hyun, G. Hauer, P. Pongratz and E. Bertagnolli, *Nano letters*, 2008, **8**, 2310–2314.

15 Y. Hyun, A. Lugstein, M. Steinmair, E. Bertagnolli and P. Pongratz, *Nanotechnology*, 2009, **20**, 5606–12.

16 K. Schwarz, J. Tersoff, S. Kodambaka, Y. Chou and F. Ross, *Physical review letters*, 2011, **107**, 5502–7.

17 Y. Wang, V. Schmidt, S. Senz and U. Gösele, *Nature nanotechnology*, 2006, **1**, 186–189.

18 P. Madras, E. Dailey and J. Drucker, *Nano letters*, 2009, **9**, 3826–3830.

19 J. Woodruff, J. Ratchford, I. Goldthorpe, M. Paul and C. Chidsey, *Nano letters*, 2007, **7**, 1637–1642.

20 J. Schmidtbauer, R. Bansen, R. Heimburger, T. Teubner, T. Boeck and R. Fornari, *Applied Physics Letters*, 2012, **101**, 043105.

21 P. Chen, J. Gaydos and A. W. Neumann, *Langmuir*, 1996, **7463**, 5956–5962.

22 K. Schwarz and J. Tersoff, *Nano letters*, 2012, **12**, 1329–1332.

23 J. Schmidtbauer, R. Bansen, R. Heimburger, T. Teubner, T. Boeck and R. Fornari, *Applied Physics Letters*, 2012, **101**, 3105–10.

24 H. Adhikari, A. Marshall, C. Chidsey and M. Paul, *Nano letters*, 2006, **6**, 318–323.

25 M. I. den Hertog, J.-L. Rouviere, F. Dhalluin, P. J. Desré, P. Gentile, P. Ferret, F. Oehler and T. Baron, *Nano letters*, 2008, **8**, 1544–50.

26 F. Oehler, P. Gentile, T. Baron and P. Ferret, *Nanotechnology*, 2009, **20**, 475307.

27 J. Hannon, S. Kodambaka, F. Ross and R. Tromp, *Nature*, 2006, **440**, 69–71.

28 F. M. Ross, *Reports on Progress in Physics*, 2010, **73**, 114501.

29 C. Wiethoff, F. Ross, M. Copel, M. Horn-von Hoegen and F. Meyer Zu Heringdorf, *Nano letters*, 2008, **8**, 3065–3068.

30 F. M. Ross, J. Tersoff and M. C. Reuter, *Physical Review Letters*, 2005, **95**, 1–4.

31 V. Dubrovskii, G. Cirlin and V. Ustinov, *Semiconductors*, 2009, **43**, 153984.

32 L. Froberg, W. Seifert and J. Johansson, *Physical Review B*, 2007, **76**, 3401–04.

33 V. Dubrovskii and N. Sibirev, *Journal of Crystal Growth*, 2007, **304**, 504–513.

34 V. Dubrovskii, T. Xu, Y. Lambert, J. Nys, B. Grandidier, D. Stiévenard, W. Chen and P. Pareige, *Physical review letters*, 2012, **108**, 5501–5.

35 J. Villain and A. Pimpinelli, *Eyrolles*, 1994.

36 J. Miguel, A. Sanchez, A. Cebollada, J. Gallego, J. Ferron and S. Ferrer, *Surface Science*, 1987, **190**, 1062–1068.

37 T. Irisawa and Y. Arima, *Journal of Crystal Growth*, 1990, **99**, 491–495.

38 V. Dubrovskii, N. Sibirev, G. Cirlin, A. Bouravleuv, Y. Samsonenko, D. Dheeraj, H. Zhou, C. Sartel, J. Harmand, G. Patriarche and F. Glas, *Physical Review B*, 2009, **80**, 5305–13.

39 V. Dubrovskii, N. Sibirev, G. Cirlin, M. Tchernycheva, J. Harmand and V. Ustinov, *Physical Review E*, 2008, **77**, 1606–13.

40 F. Oehler, P. Gentile, T. Baron, P. Ferret, M. D. Hertog and J. Rouvière, *Nano letters*, 2010, **10**, 2335–41.